Calibration of second-order correlation functions for nonstationary sources with a multistart, multistop time-to-digital converter

Wonshik Choi, Moonjoo Lee, Ye-Ryoung Lee, Changsoon Park, Jai-Hyung Lee, and Kyungwon An[a)]
School of Physics, Seoul National University, Seoul, 151-742, Korea

C. Fang-Yen, R. R. Dasari, and M. S. Feld
G. R. Harrison Spectroscopy Laboratory, Massachusetts Institute of Technology, Cambridge, Massachusetts 02139

(Received 16 March 2005; accepted 29 May 2005; published online 22 July 2005)

A novel high-throughput second-order correlation measurement system is developed that records and makes use of all the arrival times of photons detected at both start and stop detectors. This system is suitable, particularly for a light source having a high photon flux and a long coherence time, since it is more efficient than conventional methods by an amount equal to the product of the count rate and the correlation time of the light source. We have used this system in carefully investigating the dead time effects of detectors and photon counters on the second-order correlation function in the two-detector configuration. For a nonstationary light source, a distortion of the original signal was observed at high photon flux. A systematic way of calibrating the second-order correlation function has been devised by introducing the concept of an effective dead time of the entire measurement system. © *2005 American Institute of Physics.* [DOI: 10.1063/1.1986969]

I. INTRODUCTION

A second-order correlation function is an intensity-intensity correlation function, having information on both photon statistics and dynamics of the light generation process of a light source. It was first introduced by Hanbury Brown and Twiss in order to measure the angular separation of binary stars,[1] and later it was applied to the property measurement of various light sources such as measuring the coherence time of thermal light,[2] getting information on the nature of scatterers,[3] and surveying the correlation properties of laser light near the laser threshold.[4] More recently, it was used in probing the nonclassical nature of light such as antibunching[5] and sub-Poissonian photon statistics.[6]

Much effort has been made in devising a precise and efficient apparatus to measure the second-order correlation function. The first successful time-resolved measurement was done by using a single detector, a single variable delay generator, and a coincident circuit to measure the coherence time in the low-pressure gas discharge of a mercury isotope.[2] This technique has a limitation in getting the correct correlation function near the zero time delay due to the faultiness of the detector, such as spurious multiple pulse emission and the incapability of detection for a finite amount of time just after detecting a real photon. These effects are referred to as after-pulsing and dead time effects, respectively.

To overcome this limitation, a two-detector configuration has been devised in which a light beam is split into two beams, and photons in each beam are detected by each photodetector.[7–10] Unlike the single-detector configuration, the spurious photons and dead photons at one detector are completely uncorrelated to the photons detected on the other detector so that the contribution of after-pulsing and dead time effects are equally spread over the entire measurement time. This allows measurements to be extended down to the zero time delay.

More sophisticated correlators, which made use of multiple time delays, were developed that digitized the time interval between a *start* pulse from one photodetector and multiple *stop* pulses from the other photodetector at a time.[11–13] The number of pulse pairs corresponding to a given time delay is registered on a corresponding counter and the result is proportional to the second-order correlation function. Such a device is called a multistop time-to-digital converter (MSTDC). This method is more efficient than the preceding methods, owing to the multiple delay generators.

Even though a two-detector configuration can effectively remove the artifacts caused by the faultiness of the detector, this benefit is true only for a stationary source, the intensity of which is independent of time. Since the probability of spurious emissions or losing photons due to the detector dead time depends on the intensity, the measured intensity profile can be greatly distorted for a nonstationary source. In other words, the spurious emissions or lost photons are not equally spread over the entire measurement time but dependent on time. This can cause distortion in the second-order correlation measurement.

In the present study, we have carefully investigated the limitation of the two-detector configuration for nonstationary sources and have devised a systematic way of calibrating the second-order correlation function for the first time to our knowledge. For this study, we have developed a novel second-order correlation measurement system that records all the arrival times of photons detected at start and stop detec-

a)Electronic mail: kwan@phya.snu.ac.kr

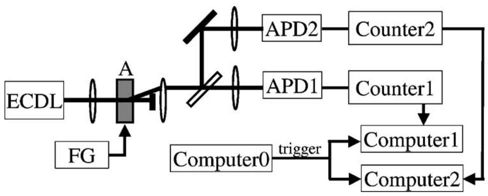

FIG. 1. Schematic of experimental setup. ECDL: Extended cavity diode laser (2010M:Newport); A: Acousto-optic modulator (Isomat 1206C); FG: Function generator (DS345, Stanford Research System); APD 1,2: Avalanche photodiode (SPCM-AQR-13, PerkinElmer); counters 1,2: NI 6602 counter/timing board. Counter/timing boards are installed in computer 1 and computer 2 separately, and are simultaneously armed by a trigger signal generated from computer 0.

tors and makes use of all the photons detected at the start detector as triggers. There is no waste of photons at the start detector, and thus our system can be much more efficient than MSTDC for a light source having a high photon flux and a long coherence time.

II. EXPERIMENTAL APPARATUS

A schematic of our second-order correlation measurement system is shown in Fig. 1. Photons are detected by two avalanche photodiodes (APDs, model SPCM-AQR-13 by Perkin Elmer). One detector (APD1) serves as a start detector while the other (APD2) serves as a stop detector. Each APD has a dark count rate of less than 150 cps and a dead time of about 50 ns and generates electrical pulses whenever the photons are detected with a detection efficiency of about 50%. APDs are electrically connected to the counter/timing boards (counters 1, 2) installed separately in two computers (computers 1, 2).

Relatively low-cost and commercially available counter/timing boards (PCI-6602 by National Instruments) are used to record the arrival times of the electrical pulses from APDs and to store them into the computers. The counter/timing board counts the number of internal clock cycles since it is armed by a trigger signal. Upon the receipt of an active edge of each electrical pulse from APD, it saves the number of clock cycles up to that instance into a save register of the board and then transmits the contents of the register to the computer memory via direct memory access (DMA). Since each board has its own internal clock of 80 MHz, the time resolution is 12.5 ns.

The counter/timing boards are installed in separate computers in order to prevent crosstalks and to maximize the data transfer rate. Although the counter/timing board has multiple input channels, only one channel per board can be used due to the significant interchannel crosstalks, which can cause a distortion of the second-order correlation function near the zero time delay. In addition, since the bandwidth of the DMA channel is limited, the simultaneous installation of two boards in a single computer would result in a reduction of the data transfer rate of each board by a factor of 2 compared to the present installation of two boards in two separate computers.

The internal clock of each counter/timing board has a limited accuracy and also has a drift of 50 ppm as the surrounding temperature changes. The accurate frequency of the internal clock in each board has been calibrated by counting the arrival times of reference pulses from the function generator (DS345, Stanford Research System). The frequency difference between boards is typically several tens of ppm and is accounted for in obtaining absolute arrival times from the measured ones.

To make the two counters start to count at the same time, an additional control computer (computer 0) is used to generate a trigger signal to simultaneously arm the counters. It has a board with analog outputs and digital inputs/outputs (NI6703, National Instruments), which can send a TTL signal as a trigger.

All the arrival times of photons detected on both detectors are the relative times with respect to the same origin defined by the trigger. All the detected photons on one detector therefore can be used as start pulses with respect to those of the other detector. For this reason, we call our apparatus a *multistart multistop time-to-digital converter* (MMTDC) compared to the conventional *multistop time-to-digital converter* (MSTDC).

MMTDC makes use of all the photons detected at a start detector whereas the MSTDC makes use of a single photon detected at a start detector as a trigger and measures the relative arrival times for a time interval that is several times (let us say n times) longer than a correlation time T_c of a light source. It starts over and repeats the next measurement cycle using another single photon detected at the start detector after nT_c. If the incoming photon flux to the start detector is γ, only one photon out of $n\gamma T_c$ photons is used in the measurement. Therefore, our MMTDC has an efficiency $n\gamma T_c$ times higher than that of MSTDC.

MMTDC is especially advantageous for a light source that has a high photon flux and a long correlation time, but has a limited operation time with its second-order correlation signal embedded in a large background. The microlaser[14,15] was a good example to fit this category. It had an output photon flux of about 3 Mcps and a correlation time of about 10 μs, such that our new method was about 30 times more efficient than that of MSTDC. Because of a limited oven lifetime, a full time measurement could give a signal-to-noise ratio of about 3, even when MMTDC was used. We could have obtained a signal-to-noise ratio of only 0.55 if we had used the conventional MSTDC method, only to fail to resolve the signal.

Due to a limitation in computer memory, the number of arrival times recordable at a time is limited by about one million counts in our MMTDC setup. To get an enough number of data, measurements should be repeated in a sequential way. All computers are connected by ethernet connections in such a way that they can send and receive messages among themselves. Whenever the counting computer (computer 1 or 2) completes a counting sequence comprising a specified number of counting events, it records the counting results on a local hard drive, prepares a next sequence, and then sends a message to the control computer in order to notify the end of the counting sequence. Upon receipt of the message from both counting computers, the control computer sends a trigger signal to them simultaneously in order to initiate a new

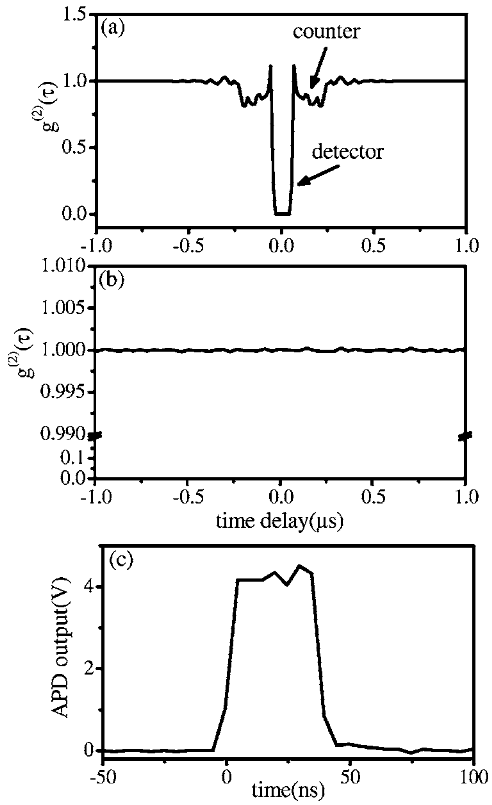

FIG. 2. (a) Second-order correlation function for a Poissonian light source measured in the single-detector configuration. (b) The same measured in the two-detector configuration. (c) The shape of a single-photon pulse from APD.

counting sequence. The number of counting sequences is determined so as to get an adequate signal-to-noise ratio.

To get the second-order correlation function, a histogram is constructed for the time differences between all possible pairs made of one of the photon arrival times at start APD and another one at stop APD. To save calculation time, only the pairs of photons the time difference of which are within a certain time window, typically chosen ten times larger than the correlation time of the source, are included in the calculation. The second-order correlation function can then be obtained from the normalization of this histogram by the averaged histogram value for much longer delay times than the correlation time.

III. EXPERIMENTS WITH STATIONARY SOURCES

We have tested our MMTDC system using an extended cavity diode laser (2010M, Newport) operating far above threshold as a test source. The photon statistics of its output is supposedly Poissonian and the second-order correlation function is thus unity for all delay times. The photon flux was 3 Mcps for each detector and the number of sequences was 1000 with 500 kilocounts per sequence.

A correlation function obtained from the photons measured at a *single* detector exhibits the effect of detector dead time and after-pulsing. Figure 2(a) shows a measured result. Two types of dip below 1 appear and the one near the zero time delay corresponds to the detector dead time. This can be confirmed from the output pulse shape of APD shown in Fig. 2(c). The full width of the pulse was measured to be about 50 ns. The stop photons following a given start photon within this time window are completely ignored and thus a dip with a depth of unity appears.

Another dip is extended to 250 ns and its depth is about 0.25, which means that the following stop photons are partially ignored with a probability of 25%. This dip originates from the counter/timing board. Usually counter electronics also have dead times since it takes a finite amount of time to record measured arrival times. In our case, since there is no onboard memory in the counter/timing board, it has to transmit the arrival times to the computer memory through DMA. Since the data transfer rate through DMA is limited by 100 MBps, some counts can be missed if the time interval between photons is too short to be transferred. The probability of missing a count depends on the time interval between successive photons. We call this loss of counts the *dead time effect of the counter* as an analogy to the detector dead time.

The correlation function obtained from the photons detected at *two* detectors is shown in Fig. 2(b). The effect of the detector and counter dead time is completely removed and the value of the correlation was very close to unity for all delay times, as expected. Since the number of photon pairs per bin amounted to 10^8, the standard deviation from unity was only 10^{-4}. Utilizing all the photons detected at the start detector helped to reduce the background noise greatly.

IV. EXPERIMENTS WITH NONSTATIONARY SOURCES

Using our MMTDC second-order correlation measurement system, we have measured the second-order correlation function for a nonstationary light source. The output beam from an extended cavity diode laser was modulated by an acousto-optic modulator. The amplitude of a driving rf field to the acousto-optic modulator was sinusoidally modulated using a function generator so that the intensity of the first-order diffracted beam was sinusoidally modulated. Its functional form can be written as $I(t)=a\sin(\omega t+\phi)+b$, where a and b have the units of counts per second for the photon counting measurement. Since the response time of AOM is measured to be 130 ns, the modulation frequency can be safely set up to 1 MHz. For the present experiments, the modulation frequency was set as 100 kHz.

The normalized second-order correlation function for a classical source, applied to the intensity of electromagnetic field $I(t)$ is given by

$$g^{(2)}(\tau)=\frac{\langle I(t)I(t+\tau)\rangle}{\langle I(t)\rangle^2}, \tag{1}$$

where $\langle\ldots\rangle$ denotes the time average. The second-order correlation function for the sinusoidally modulated source is thus calculated to be

$$g^{(2)}(\tau)=1+\frac{a^2}{2b^2}\cos\omega\tau. \tag{2}$$

Figures 3(a) and 3(b) show measured second-order correlation functions. The mean count rates for individual detectors were about 0.6 Mcps and 1000 sequences of measurements

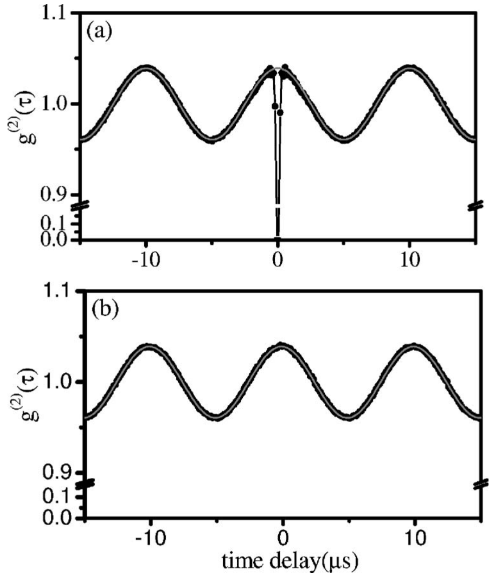

FIG. 3. Typical result of the second-order correlation function for a sinusoidally modulated light source measured in (a) a single-detector configuration and (b) a two-detector configuration.

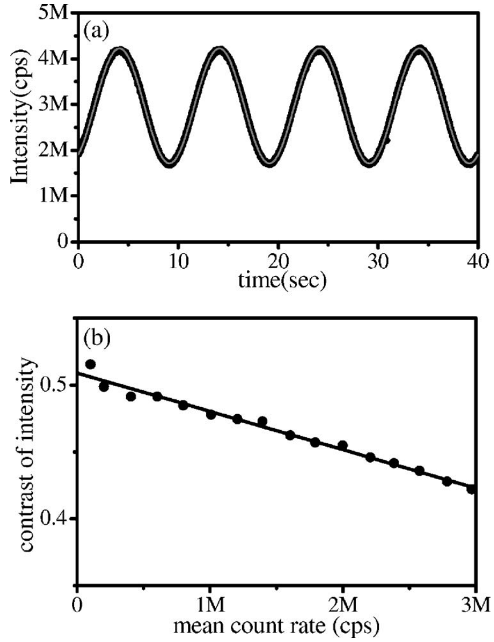

FIG. 4. (a) Intensity profile of a sinusoidally modulated light source measured by the photon counting method. (b) Contrasts of the intensity. Circular dots: the measured contrast ratio from fitting the intensity; line: theoretical calculation including the effect of the detector dead time of 56 ns.

were done with each sequence counting 300 kilocounts for each detector. It took about 1000 s, including a sequencing procedure. The adjacent points were added up and thus the time resolution was 125 ns.

Figure 3(a) is the second-order correlation function obtained from photons detected at a single detector and thus shows a sharp dip near time delay zero. The dip results from the dead times of the detector and the counter. On the other hand, Fig. 3(b) is obtained from the photons detected on two detectors, APD1 and APD2. The central dip is completely eliminated, as in the case of stationary light sources. The normalized shot noise is only about 0.06% due to the large mean counts per bin of about 2.8 million. The contrast ratios $a^2/2b^2$ of single- and two-detector configurations are almost the same.

A. Dead time effect on nonstationary intensity

Even though the two-detector configuration can eliminate the detector dead time effect near the zero time delay, the detector dead time still can affect the correlation measurements for nonstationary sources when the detector counting rate becomes comparable to the inverse of the detection dead time. Since the probability to miss photons is dependent on the intensity, the measured time-varying intensity profile can be distorted.

We used a photon counting method to measure the time-dependent intensity. Since our MMTDC was based on the photon counting method, we used a photon counting technique rather than a photocurrent measurement for a consistent quantitative relation between the intensity profile and the second-order correlation function. In order to obtain an adequate number of counts per counting bin for an intensity measurement, which has to be done in a fashion of a single shot measurement, we used a slow intensity modulation frequency of 0.1 Hz for a given incoming photon flux of around 1 MHz.

Photons were counted for every counting bin of 0.01 s and the counted numbers were transferred at the end of each bin. Since the dead time of the counter occurs when the time interval between successive data transfers is shorter than 250 ns, this measurement should be free from the counter dead time effect. At a 1 MHz counting rate, the mean counts N per bin were 10^4 counts and thus the normalized noise $\sqrt{N}/N$ was 0.01, which means we could resolve an intensity modulation whose contrast was as small as 0.01.

We repeated the measurement for various mean count rates b while keeping the contrast of the intensity a/b constant. To do so, we fixed the radiofrequency field driving the acousto-optic modulator and varied the mean intensity using neutral density filters. The intensities measured in this way were well fitted by sinusoidal functions as shown in Fig. 4(a). The contrast ratio in Fig. 4(a) is about 0.422, which corresponds to the contrast ratio at a mean intensity of 3 Mcps in Fig. 4(b), where the measured results denoted by circular dots show a linear decrease as the mean count rate increases.

This linear decrease can be explained in terms of the correction factor α of the detector, which needs to be multiplied by the measured intensity to get an original intensity,

$$\alpha = \frac{I}{I_m} = 1 + T_d I, \tag{3}$$

where I and I_m are the original and measured intensities, respectively, in units of cps and T_d is the dead time of the detector. If there exists additional dead times, such as the dead time of the counting board, T_d should be replaced with an effective total dead time including all dead times, and this subject will be discussed in detail in the next section. For $T_d a \ll 1$ and $T_d b \ll 1$,

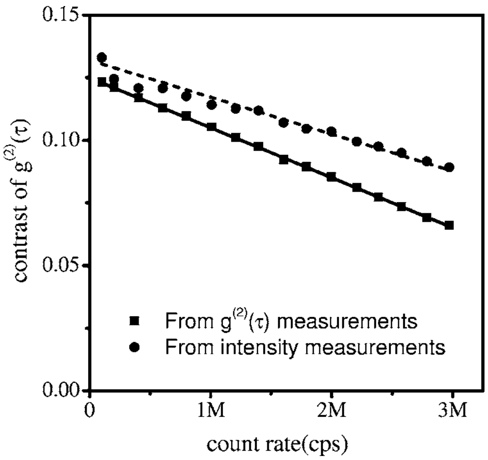

FIG. 5. Contrast of the second-order correlation function. Square dots: calculated from the measured $g^{(2)}(\tau)$ (100 kHz); circular dots: expected from the measured contrasts of the intensity (0.1 Hz modulation). Solid and dashed lines are theoretical results with the effective dead time of 80 ns and 56 ns, respectively.

$$I_m(t) \simeq [1 - T_d I(t)]I(t) \simeq b - T_d b^2 + (a - 2abT_d)\sin \omega t \simeq b(1 - T_d b)[1 + (a/b)(1 - T_d b)\sin \omega t], \quad (4)$$

which shows that the contrast ratio is modified from a/b to $(1-T_d b)(a/b)$.

Note that the unmodified contrast a/b, fixed in the experiment, can be determined from the y intercept of a linear fit to the measured contrast ratios, and the inclination of the linear fit corresponds to the dead time T_d. In Fig. 4(b), we get $a/b \simeq 0.5$ and $T_d \simeq 56$ ns, which is about 10% larger than our initial estimate based on the single-photon pulse shape in Fig. 2(b). This discrepancy is due to the finite bin size of 12.5 ns, which results in an additional broadening of about 6 ns, half the bin size, in the effect of the detector dead time in the correlation function.

B. Dead time effect on $g^{(2)}(\tau)$

Since the intensity profile is distorted by the detector dead time, the second-order correlation function will be also affected. For a measured intensity contrast of a'/b', the expected contrast of the second-order correlation function is $a'^2/2b'^2$.[16] They are denoted by circular dots in Fig. 5. For an unmodified contrast a/b, the dependence of the measured contrast a'/b' on the mean intensity b is given by $(1-T_d b)a/b$. The contrast of $g^{(2)}(\tau)$ is thus expected to be

$$a'^2/2b'^2 = \frac{1}{2}[(1 - T_d b)(a/b)]^2 \simeq (1 - 2T_d b)a^2/2b^2. \quad (5)$$

The dashed line in Fig. 5 indicates the expected contrast with T_d=56 ns.

Using MMTDC, we have measured the second-order correlation function under the condition identical to the one under which we had measured the intensity, except for the intensity modulation frequency, which is now set at 100 kHz, since the correlation measurement need not be done in a single-shot fashion, as in the intensity measurement. The square dots in Fig. 5 are the contrasts obtained by fitting the measured $g^{(2)}(\tau)$ with a sinusoidal function. It decreases linearly as the photon flux increases, but the decreasing rate of the contrast ratio is 1.54 times larger than that expected from the intensity measurement.

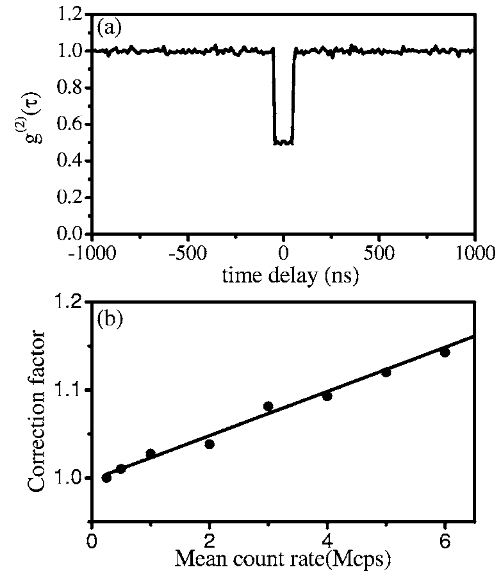

FIG. 6. The numerical simulation result for a partial dead time effect. A dead time of 50 ns and the probability of losing a photon of 0.5 are assumed. (a) A second-order correlation function. (b) Correction factors as a function of the mean count rate of incoming photons. The solid line is a linear fit.

This discrepancy is due to the dead time of the counter/timing board, which was absent in the preceding intensity measurement performed at 0.1 Hz modulation frequency with a data transfer rate of 100 Hz. In the second-order correlation measurement, regardless of the modulation frequency, since all of the arrival times are recorded, the data transfer rate can be much faster than the inverse of 250 ns, which is the maximum dead time of the counter. When the time difference of two successive photons is shorter than 250 ns, there exists a finite chance that the following photon is ignored. A complexity arises since this chance is not always unity. It can be anywhere between 0 and 1. We thus need to find an effective dead time that can properly include both detector and counter dead time effects.

V. ANALYSIS AND CALIBRATION METHOD

To understand the dead time effect of a counter, we numerically simulated the effect of a partial dead time. A Poissonian light source was simulated using a random number generation algorithm. In the simulation, if the time difference between two successive photons are shorter than 50 ns, the following photon is omitted with a probability P_L of 50%. This probability would be unity for the case of the detector dead time. Figure 6(a) is the second-order correlation function of this simulated source and shows a dip with a half-width the same as the dead time and a depth equal to P_L, 50%. The correction factor α is calculated as a function of the mean intensity and is shown in Fig. 6(b). The result can be well fitted by the following relation:

$$\alpha = \frac{I}{I_m} = 1 + P_L T_d I. \quad (6)$$

Note that the linearity coefficient in α with respect to the intensity is not T_d, as in Eq. (3), but $P_L T_d$. We can generalize this observation and expect that the detector dead time T_d in Eq. (5) will be replaced by $P_L T_d$. This expectation has been confirmed by our numerical simulations. Therefore, we call $T_{\text{eff}} \equiv P_L T_d$ an effective dead time, and it is equal to the area of the dip ($\tau \geqslant 0$ only) around the origin in the second-order correlation function obtained in the single-detector configuration [Fig. 6(a)]. In general, we can experimentally determine the effective dead time $T_{\text{eff}}^{(\text{tot})}$ of an entire detection system from the dead time distribution, i.e., the shape of the second-order correlation function around the origin, calculated with photons detected on a single detector only.

The dead time distribution of our MMTDC system is shown in Fig. 2(a). The total area of the dip near the origin is 80 ns, which is our effective dead time $T_{\text{eff}}^{(\text{tot})}$ for the entire measurement system. The area of the central dip only equals T_d=55 ns, originating from the detector dead time. The ratio $T_{\text{eff}}^{(\text{tot})}/T_d$ is 1.45, and thus we expect that the inclination of the observed contrast in $g^{(2)}(\tau)$ with respect to the counting rate b would be 1.45 times greater than that expected from the intensity measurement free from the counter dead time effect. This is what we have observed in Fig. 5, where the observed ratio is 1.54, showing only a 6% discrepancy from our expectation.

From these observations, we can establish a calibration method for the second-order correlation function of a nonstationary light source. We first measure the second-order correlation function using the single detector configuration and determine the effective dead time $T_{\text{eff}}^{(\text{tot})}$ of the entire system from the dead time distribution around the origin. The second-order correlation function is then measured again, but this time in the two detector configuration. Since the correction factor in Eq. (6) is independent of the modulation frequency, we can calibrate the measured correlation function by dividing its amplitude by $(1-2T_{\text{eff}}^{(\text{tot})}b)$, where b is the mean count rate.

ACKNOWLEDGMENTS

This work was supported by Korea Research Foundation Grant No. KRF-2002-070-C00044, a grant from the Ministry of Science and Technology (MOST) of Korea, and NSF Grant No. 9876974-PHY.

[1] E. Hanbury Brown and R. Q. Twiss, Nature (London) **177**, 27 (1957).
[2] B. L. Morgan and L. Mandel, Phys. Rev. Lett. **16**, 1012 (1966).
[3] H. Z. Cummins and H. L. Swinney, in *Progress in Optics*, edited by E. Wolf (North-Holland, Amsterdam, 1970), Vol. 8, p. 133.
[4] F. T. Arecchi, E. Gatti, and A. Sona, Phys. Lett. **20**, 27 (1966).
[5] H. J. Kimble, M. Dagenais, and L. Mandel, Phys. Rev. Lett. **39**, 691 (1977).
[6] R. Short and L. Mandel, Phys. Rev. Lett. **51**, 384 (1983).
[7] D. B. Scarl, Phys. Rev. Lett. **17**, 663 (1966).
[8] D. T. Phillips, H. Kleiman, and S. P. Davis, Phys. Rev. **153**, 113 (1967).
[9] F. Davidson and L. Mandel, J. Appl. Phys. **39**, 62 (1968).
[10] F. Davidson, Phys. Rev. **185**, 446 (1969).
[11] H. Z. Cummins and E. R. Pike, *Photon Correlation Spectroscopy and Velocimetry* (Plenum, New York, 1977).
[12] H. L. Swinney, Physica D **7**, 3 (1983).
[13] E. R. Pike, in *Coherence, Cooperation and Fluctuations* (Cambridge University Press, Cambridge, 1986), p. 293.
[14] K. An, J. J. Childs, R. R. Dasari, and M. S. Feld, Phys. Rev. Lett. **73**, 3375 (1994).
[15] W. Choi, J.-H. Lee, K. An, C. Fang-Yen, R. R. Dasari, and M. S. Field (in preparation).
[16] D. Meschede, H. Walther, and G. Muller, Phys. Rev. Lett. **54**, 551 (1985).